

# CrystEngComm

## Accepted Manuscript



This is an *Accepted Manuscript*, which has been through the RSC Publishing peer review process and has been accepted for publication.

*Accepted Manuscripts* are published online shortly after acceptance, which is prior to technical editing, formatting and proof reading. This free service from RSC Publishing allows authors to make their results available to the community, in citable form, before publication of the edited article. This *Accepted Manuscript* will be replaced by the edited and formatted *Advance Article* as soon as this is available.

To cite this manuscript please use its permanent Digital Object Identifier (DOI®), which is identical for all formats of publication.

More information about *Accepted Manuscripts* can be found in the [Information for Authors](#).

Please note that technical editing may introduce minor changes to the text and/or graphics contained in the manuscript submitted by the author(s) which may alter content, and that the standard [Terms & Conditions](#) and the [ethical guidelines](#) that apply to the journal are still applicable. In no event shall the RSC be held responsible for any errors or omissions in these *Accepted Manuscript* manuscripts or any consequences arising from the use of any information contained in them.

Cite this: DOI: 10.1039/c0xx00000x

www.rsc.org/xxxxxx

ARTICLE TYPE

# Structural competition between $\pi\cdots\pi$ interaction and halogen bond: a crystallographic study†

Baoming Ji,<sup>a\*</sup> Weizhou Wang,<sup>a</sup> Dongsheng Deng,<sup>a</sup> Yu Zhang,<sup>a</sup> Lei Cao,<sup>ab</sup> Le Zhou,<sup>b</sup> Chuansheng Ruan<sup>ac</sup> and Tiesheng Li<sup>c</sup>

<sup>5</sup> Received (in XXX, XXX) Xth XXXXXXXXXX 20XX, Accepted Xth XXXXXXXXXX 20XX  
DOI: 10.1039/b000000x

1,3-Diiodotetrafluorobenzene and 1,3,5-trifluoro-2,4,6-triiodobenzene form cocrystals with 4,4',6,6'-tetramethyl-2,2'-bipyrimidine, 1,2,4,5-tetra(3-pyridyl)benzene and 1,2,4,5-tetra(4-pyridyl)benzene in which the structural competition between  $\pi\cdots\pi$  interaction and halogen bond is directly observed. It is found that the strong C–I $\cdots$ N halogen bond competes successfully with the  $\pi\cdots\pi$  interaction between two 1,3-diiodotetrafluorobenzene molecules while the  $\pi\cdots\pi$  interaction between two 1,3,5-trifluoro-2,4,6-triiodobenzene molecules can successfully compete with the strong C–I $\cdots$ N halogen bond. Quantum chemical calculations explain the structural competition well.

## Introduction

15 The number of crystal structures, in which intermolecular interactions have been reported to play key roles, has grown rapidly in recent years.<sup>1–3</sup> These intermolecular interactions include: hydrogen bonds,<sup>1</sup>  $\pi\cdots\pi$  interactions,<sup>2</sup> halogen bonds,<sup>3</sup> van der Waals forces, etc. Evidently, crystal structures cannot be rationalized and predicted from considerations of only one type of intermolecular interaction and different types of interactions should be considered jointly in structure analysis. This puts difficulties in the way of the design and construction of molecular architectures with desirable connectivity and precisely defined metrics. The only way to overcome such difficulties is to identify the competition between the directional or nondirectional intermolecular interactions of different strength.<sup>4</sup>

Besides the hydrogen bond, the  $\pi\cdots\pi$  interaction also occurs frequently and makes a substantial contribution to the crystal packing.<sup>2</sup> Another important noncovalent driving force for supramolecular assembly is the halogen bond.<sup>3</sup> In supramolecular chemistry and especially in crystal engineering involving the halogen bond, aryl or heteroaryl iodide is often used as the halogen atom donor.<sup>4</sup> Along with the formation of the halogen bond between the aryl or heteroaryl iodide and the electron density donor, the  $\pi\cdots\pi$  interaction is routinely observed between the homogeneous dimer of the aryl or heteroaryl iodide. However, the structural competition between  $\pi\cdots\pi$  interaction and halogen bond is very seldom studied.<sup>5,6</sup> Lu and coworkers studied the interplay between  $\pi\cdots\pi$  interaction and halogen bond employing the Cambridge Structural Database search and theoretical computation.<sup>5</sup> However, they did not consider the  $\pi\cdots\pi$  interaction between the homogeneous dimer of the aryl or heteroaryl iodide which is the topic of the present study. In a very recent paper, we explored the competition between  $\pi\cdots\pi$  interaction and halogen bond in solution by using a combined <sup>13</sup>C

NMR and density functional theory method.<sup>6</sup> Herein, we address this issue through a series of cocrystallization reactions between 1,3-diiodotetrafluorobenzene (**1**)<sup>7</sup> or 1,3,5-trifluoro-2,4,6-triiodobenzene (**2**)<sup>8</sup> and 4,4',6,6'-tetramethyl-2,2'-bipyrimidine (**a**),<sup>9</sup> 1,2,4,5-tetra(3-pyridyl)benzene (**b**)<sup>10</sup> or 1,2,4,5-tetra(4-pyridyl)benzene (**c**)<sup>11</sup> (Fig. 1).

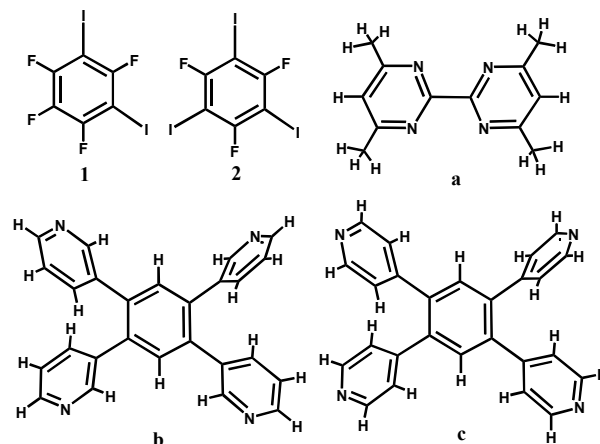


Fig. 1 The **1** and **2**, investigated as cofomers with the **a**, **b** and **c**.

## Experimental

### Materials and general methods

All reagents and chemicals, except where indicated, were purchased from commercial sources and were used without further purification. NMR experiments were performed using a Bruker Avance spectrometer. <sup>1</sup>H NMR spectra were recorded at 400 MHz. <sup>13</sup>C NMR spectra were recorded at 100 MHz. The **1**, **2** and **a** were prepared by the methods reported previously.<sup>7–9</sup>

**Synthesis of b.** A mixture of 1,2,4,5-tetrabromobenzene (3.74 g, 10.0 mmol), pyridin-3-ylboronic acid (7.40 g, 10.0 mmol),

Cite this: DOI: 10.1039/c0xx00000x

www.rsc.org/xxxxxx

## ARTICLE TYPE

**Table 1.** Crystallographic data and structure refinement parameters for **1a**, **2a**, **1b**, **2b**, **1c** and **2c**.

	<b>1a</b>	<b>2a</b>	<b>1b</b>	<b>2b</b>	<b>1c</b>	<b>2c</b>
Empirical formula	C <sub>18</sub> H <sub>13</sub> F <sub>4</sub> I <sub>2</sub> N <sub>4</sub>	C <sub>54</sub> H <sub>28</sub> F <sub>15</sub> I <sub>15</sub> N <sub>8</sub>	C <sub>32</sub> H <sub>18</sub> F <sub>4</sub> I <sub>2</sub> N <sub>4</sub>	C <sub>38</sub> H <sub>18</sub> F <sub>6</sub> I <sub>6</sub> N <sub>4</sub>	C <sub>39</sub> H <sub>19</sub> Cl <sub>3</sub> F <sub>8</sub> I <sub>4</sub> N <sub>4</sub>	C <sub>38</sub> H <sub>18</sub> F <sub>6</sub> I <sub>6</sub> N <sub>4</sub>
formula weight	616.13	2977.34	788.30	1405.96	1322.55	1405.96
crystal size (mm <sup>3</sup> )	0.40×0.22×0.19	0.45×0.28×0.21	0.41×0.22×0.20	0.35×0.31×0.28	0.43×0.21×0.18	0.35×0.27×0.25
crystal system	monoclinic	triclinic	triclinic	triclinic	monoclinic	triclinic
space group	<i>P</i> 2 <sub>1</sub> / <i>c</i>	<i>P</i> $\bar{1}$	<i>P</i> $\bar{1}$	<i>P</i> $\bar{1}$	<i>C</i> 2/ <i>c</i>	<i>P</i> $\bar{1}$
<i>a</i> /Å	7.5669(8)	9.2428(9)	9.2000(11)	8.9547(11)	20.9771(19)	9.3457(10)
<i>b</i> /Å	24.046(3)	11.0863(11)	9.4032(11)	11.1438(14)	20.4699(18)	10.8381(11)
<i>c</i> /Å	11.6567(15)	18.8796(19)	17.302(2)	11.4320(14)	10.1640(9)	11.4689(12)
$\alpha$ /°	90	87.942(1)	82.198(1)	74.690(1)	90	114.173(1)
$\beta$ /°	108.784(1)	85.311(1)	79.011(1)	85.622(1)	95.316(1)	102.914(1)
$\gamma$ /°	90	84.428(1)	85.566(1)	69.136(1)	90	91.208(1)
volume/Å <sup>3</sup>	2008.0(4)	1918.2(3)	1453.7(3)	1028.0(2)	4345.6(7)	1024.69(19)
<i>Z</i>	4	1	2	1	4	1
$\rho_{\text{calc}}$ /g cm <sup>-3</sup>	2.038	2.577	1.801	2.271	2.021	2.278
<i>T</i> /K	296(2)	296(2)	296(2)	296(2)	296(2)	296(2)
$\theta$ range for data collection (deg)	2.51–25.50	2.39–25.50	2.37–25.50	2.37–25.49	2.37–25.50	2.61–25.50
reflections collected	14734	14235	11130	7622	15952	7614
no. unique data [ <i>R</i> (int)]	3734 [0.0252]	7082 [0.0305]	5379 [0.0226]	3791 [0.0228]	4043 [0.0206]	3779 [0.0144]
final <i>R</i> ( <i>I</i> > 2 $\sigma$ ( <i>I</i> ))	0.0271	0.0407	0.0336	0.0268	0.0318	0.0226
final <i>wR</i> <sub>2</sub> (all data)	0.0597	0.1025	0.0854	0.0659	0.1004	0.0601
goodness-of-fit	1.061	1.057	1.012	1.078	1.021	1.006

K<sub>2</sub>CO<sub>3</sub> (22.00 g, 160.0 mmol), and Pd(PPh<sub>3</sub>)<sub>4</sub> (2.00 g, 1.73 mmol) was weighed into a 500 mL Schlenk flask, to which 1,4-dioxane (240 mL) and H<sub>2</sub>O (80 mL) were added subsequently under a dry N<sub>2</sub> atmosphere. The mixture was heated to reflux with stirring and maintained at this temperature for 36 h. The reaction mixture was cooled to room temperature and diluted with CH<sub>2</sub>Cl<sub>2</sub>. The combined organic layers were washed several times with brine, dried over anhydrous Na<sub>2</sub>SO<sub>4</sub>, and then concentrated under reduced pressure. The crude product was purified by column chromatography on silica gel (1:35 CH<sub>3</sub>OH/CH<sub>2</sub>Cl<sub>2</sub>) to afford **b** (2.38 g, 61.0 % yield) as a white solid. <sup>1</sup>H NMR (CDCl<sub>3</sub>):  $\delta$  8.53 (s, 8H, ArH), 7.58 (s, 2H, ArH), 7.51 (d, *J* = 8.0 Hz, 4H, ArH), 7.22 (d, *J* = 4.0 Hz, 4H, ArH). <sup>13</sup>C NMR (CDCl<sub>3</sub>):  $\delta$  150.34, 148.71, 137.59, 137.05, 135.44, 133.15, 123.17.

**Synthesis of c.** Synthesis of **c** was the same as that of **b** except that the pyridin-4-ylboronic acid not the pyridin-3-ylboronic acid was used. The yield of **c** is about 82.0 % (3.16 g, white solid). <sup>1</sup>H NMR (CDCl<sub>3</sub>):  $\delta$  8.55 (d, *J* = 4.0 Hz, 8H, ArH), 7.55 (s, 2H, ArH), 7.14 (s, 8H, ArH). <sup>13</sup>C NMR (CDCl<sub>3</sub>):  $\delta$  150.08, 147.23, 138.58, 132.64, 124.42.

**Preparation of cocrystals**

The halogen bond donors and acceptors in a molar ratio of 1:1 were dissolved in approximately 25 mL of chloroform with gentle stirring at room temperature. The undissolved materials were removed by filtration. The filtrate was set aside for crystallization at room temperature. After a few days, the single crystals suitable for X-ray analysis were obtained.

To explore the influence of the ratio of donor to acceptor on the formation of these compounds, a series of co-crystallization experiments between halogen compound and nitrogen-containing aromatic compound were performed by altering the ratio of the two reactants from 1:1 to 1:2. It was found that the same crystals were always obtained in CHCl<sub>3</sub> regardless of donor/acceptor molar ratio of the two components. The stoichiometry of the compounds (**1a**, **2a**, **1b**, **2b**, **1c**, and **2c**) in the co-crystal is different from that of the solution. However, this is not uncommon. A similar phenomenon can be documented by recent reports by van der Boom.<sup>12</sup> In addition, as a consequence of the low solubility of the base and acid species in other organic solvent such as acetone, acetonitrile, benzene, and methanol, the

combination of them only led to the formation of a lot of precipitates. Consequently, in  $\text{CHCl}_3$ , the donor/acceptor 1:1 was selected as the optimal reaction conditions.

### X-Ray crystallography

Crystallographic data were collected on a Bruker Smart Apex-II CCD area detector equipped with a graphite-monochromatic Mo  $K\alpha$  radiation ( $\lambda = 0.71073 \text{ \AA}$ ) at room temperature. An empirical absorption correction was applied. All structures were solved and refined by a combination of direct methods and difference Fourier syntheses, using SHELXTL.<sup>13,14</sup> Anisotropic thermal parameters were assigned to all non-hydrogen atoms. The hydrogen atoms were set in calculated positions and refined as riding atoms with a common isotropic thermal parameter. The crystallographic data and structure refinement parameters are listed in Table 1.

Notably, the methyl (C9) H atoms in compound **2a** were found at the difference Fourier map and subsequently constrained with HFIX 123 constraint. In the case of C25, C26, C27, C28, C29, C30, F7, F8, I7, I8, and I9, these atoms are disordered about the mirror plane, and upon generation of the mirror symmetry, their disordered counterpart is generated. Thus, these atoms are modelled with occupancy of 50%. Further, C20, Cl1, Cl2, and Cl3 in compound **1c** were refined by using the "ISOR" restraint to make the ADP values of the disordered atoms.

X-ray powder diffraction patterns were collected at 293 K on a Bruker AXS DifractPlus D8 Advance diffractometer using a Cu generator with wavelength of the  $K\alpha, \text{Cu}$  radiation of 1.5406  $\text{\AA}$ . The  $2\theta$  angle was scanned between  $5^\circ$  and  $50^\circ$ , and the counting time was 2 seconds at each angle step ( $0.01052^\circ$ ) without using delay time (see ESI†).

### Results and discussion

Experiments have proved that the interaction between the highly polarized iodine and the nitrogen atom is strong.<sup>3a</sup> It is generally accepted that the strong halogen bond is an electrostatically-driven highly directional noncovalent interaction.<sup>15</sup> Hence, we can use the angle ( $\theta$ ) to describe the strength of halogen bond in the crystal structure: smaller values of  $\theta$  mean much stronger halogen bonds (Fig. 2). As shown below, the values of  $\theta$  are in proportional to the values of the corresponding I...N distances, which proves again the rationality of using  $\theta$  to describe the strength of halogen bond.

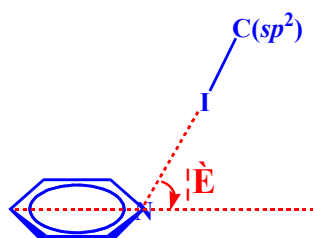


**Fig. 2** The angle ( $\theta$ ) used to describe the strength of halogen bond.

Compound **1** forms a 1:1 cocrystal with **a**, to give **1a**, in the monoclinic space group  $P2_1/c$  and **2** with **a** forms a 5:2 cocrystal **2a** in the triclinic space group  $P\bar{1}$ . In **1a**, the propagation of the

asymmetric bifurcated halogen bond constructs a 1-D chain, as depicted in Fig. 3 (top). The 1-D chains are then held together two by weak  $\text{C-H}\cdots\text{F}$  ( $\text{C13}\cdots\text{F3}$ : 3.365(2),  $154.4^\circ$ ;  $\text{C8}\cdots\text{F1}$ : 3.502(2)  $\text{\AA}$ ,  $134.9^\circ$ ) interactions, resulting in a 2-D sheet. There is no  $\pi\cdots\pi$  stacking interaction between two **1** molecules. The value of  $\theta$  shown in Fig. 3 (top) is about  $10^\circ$ , which shows little deviation from linearity. The case in **2a** is totally different from that in **1a**. The molecules organize themselves into linear ribbons through four halogen bonds and the  $\pi\cdots\pi$  stacking interactions. Perpendicular to these ribbons, the  $\pi\cdots\pi$  stacking interactions based on the **2** molecules with parallel alignment are formed which are responsible for the formation of 2-D layer structure. As shown in Fig. 3 (bottom), one halogen bond is strong ( $\theta=3^\circ$ ); the other halogen bond is very weak ( $\theta=58^\circ$ ). Evidently, it is the formation of the  $\pi\cdots\pi$  stacking interaction between two **2** molecules that makes it impossible to form two strong halogen bonds like that in **1a**. Comparing the cocrystal structures of **1a** and **2a**, we can see that the strong  $\text{C-I}\cdots\text{N}$  halogen bond competes successfully with the  $\pi\cdots\pi$  interaction between two **1** molecules while the  $\pi\cdots\pi$  interaction between two **2** molecules can successfully compete with the strong  $\text{C-I}\cdots\text{N}$  halogen bond.

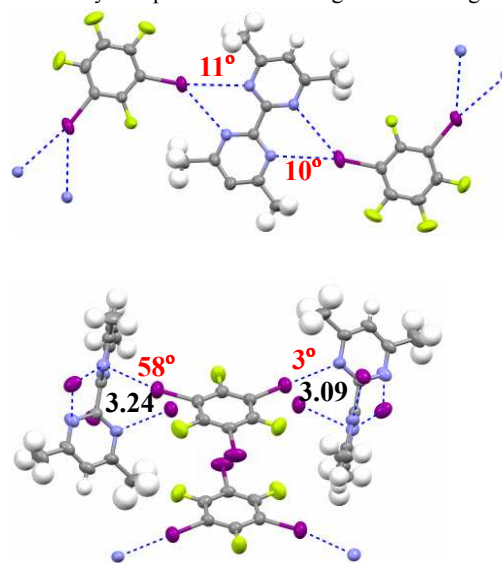


**Fig. 3** Partial view (ellipsoid representation) of the crystal packing of **1a** (top) and **2a** (bottom). Dashed lines indicate halogen bonds. Colour code: Carbon: gray; Nitrogen: blue; Fluorine: yellow; Iodine: purple; Hydrogen: light gray. The values of  $\theta$  are shown in red numbers. The corresponding I...N distances ( $\text{\AA}$ ) are shown in black numbers.

In chloroform solvent, compound **1** forms a 1:1 cocrystal with **b**, to give **1b**, in the monoclinic space group  $P\bar{1}$ , and **2** with **b** forms a 2:1 cocrystal **2b**, in the triclinic space group  $P\bar{1}$ . The structural competition between  $\pi\cdots\pi$  interaction and halogen bond in **1b** and **2b** is similar to that in **1a** and **2a** (Fig. 4). In **1b**, the  $\text{C-I}\cdots\text{N}$  halogen bonds, with the help of weak  $\text{C-I}\cdots\text{I}$  and  $\text{C-H}\cdots\text{N}$  interactions, may be effective in the stabilization of the 2-D layer structure. In order to form the strong  $\text{C-I}\cdots\text{N}$  halogen bond ( $\theta=13^\circ$ ), the molecules of **1** are separated a great distance from one another in space (distance between two ring centroids=9.485  $\text{\AA}$ ), such that there is no  $\pi\cdots\pi$  interaction between two **1** molecules. In **2b**, in order to form the  $\pi\cdots\pi$  interaction between two **2** molecules, one halogen bond ( $\theta=58^\circ$ ) becomes much

[View Online](#)

weaker than the other halogen bond ( $\theta=14^\circ$ ). The crystal structures of **1b** and **2b** also reflect the structural advantage of the strong C-I $\cdots$ N halogen bond over the  $\pi\cdots\pi$  interaction between two **1** molecules and the structural advantage of the  $\pi\cdots\pi$  interaction between two **2** molecules over the strong C-I $\cdots$ N halogen bond. Inevitably, there are many other noncovalent interactions such as C-H $\cdots$ N, C-H $\cdots\pi$  and C-I $\cdots$ I in **1b** and **2b**, but these noncovalent interactions are very weak and have little effect on the structural competition between  $\pi\cdots\pi$  interaction and halogen bond.

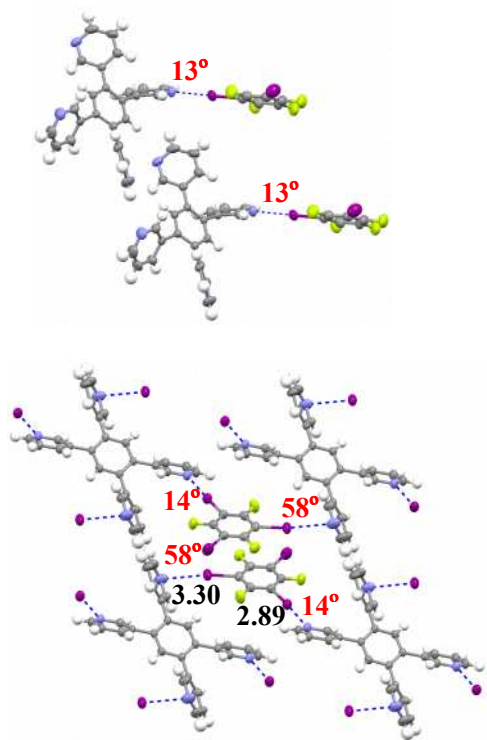


**Fig. 4** Partial view (ellipsoid representation) of the crystal packing of **1b** (top) and **2b** (bottom). Dashed lines indicate halogen bonds. Colour code: Carbon: gray; Nitrogen: blue; Fluorine: yellow; Iodine: purple; Hydrogen: light gray. The values of  $\theta$  are shown in red numbers. The corresponding I $\cdots$ N distances (Å) are shown in black numbers.

As shown in Fig. 5, the crystal packing of **1c** (the 2:1 cocrystal of **1** and **c**) is governed mainly by the strong C-I $\cdots$ N halogen bonds ( $\theta=4^\circ$  and  $\theta=12^\circ$ ). The C-I $\cdots$ N halogen bonds generate the main building blocks of the crystal. These building blocks are then organized into the 3-D structure with 1D channels along the *c* axis (Fig. 6). In the structure, C-H $\cdots$ F weak interactions can also be formed as those in cocrystal **1a**, which further consolidate the crystal packing. It is interesting to note that the 1D channels are filled with chloroform molecules. The guest molecules interact with the host also through the weak C-H $\cdots$ F hydrogen bonds. Hence, the effect of the solvent molecules on the structural competition between the strong  $\pi\cdots\pi$  interaction and the strong halogen bond can be neglected. For the **1** molecules in **1c**, the shortest distance between two ring centroids is 5.437 Å. Obviously, there is no  $\pi\cdots\pi$  interaction between two **1** molecules in **1c**. **2c** (the 2:1 cocrystal of **2** and **c**) has assembled into a 2-D sheet structure via a combination of strong C-I $\cdots$ N halogen bonds ( $\theta=8^\circ$ ), weak C-I $\cdots$ N halogen bonds ( $\theta=32^\circ$ ) and  $\pi\cdots\pi$  interactions

(Fig. 6). Again, the structural competition between  $\pi\cdots\pi$  interaction and halogen bond results in that there is no  $\pi\cdots\pi$  interaction between two **1** molecules in **1c** and the weak C-I $\cdots$ N halogen bonds ( $\theta=32^\circ$ ) exists in **2c**.

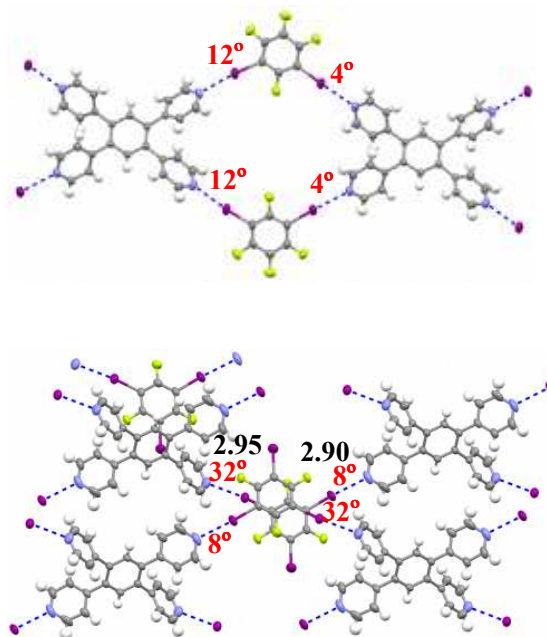


**Fig. 5** Partial view (ellipsoid representation) of the crystal packing of **1c** (top) and **2c** (bottom). Dashed lines indicate halogen bonds. Colour code: Carbon: gray; Nitrogen: blue; Fluorine: yellow; Iodine: purple; Hydrogen: light gray. The values of  $\theta$  are shown in red numbers. The corresponding I $\cdots$ N distances (Å) are shown in black numbers.

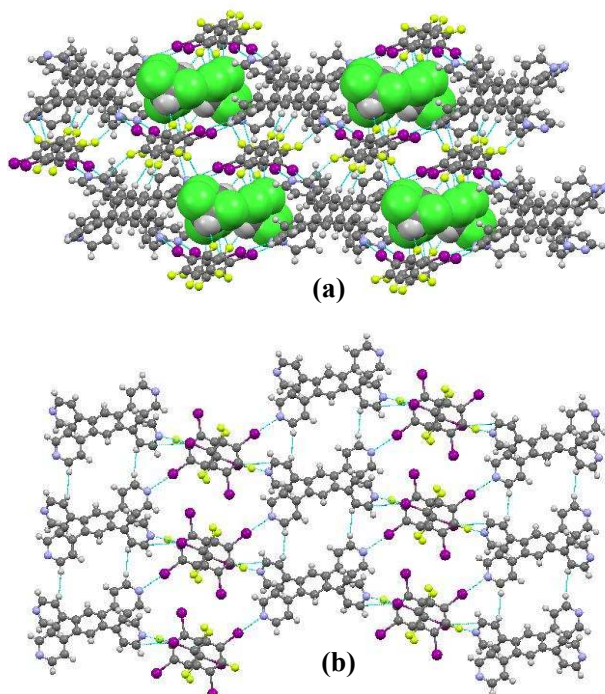


**Fig. 6.** (a) Mercury view of 3-D architecture of **1c**. The C-I $\cdots$ N and C-H $\cdots$ F interactions are indicated as blue dashed lines. (b)

Mercury view of 2-D sheet of **2c** in the *ab* plane. The C–I⋯N and C–H⋯F interactions are indicated as blue dashed lines.

For confirming the phase purity and homogeneity of the cocrystals, X-ray powder diffraction measurements for **1a**, **2a**, **1b**, **2b**, **1c** and **2c** were performed at room temperature. The peaks displayed in the measured patterns for each cocrystal closely match those in the simulated patterns generated from single-crystal diffraction data, indicating a good phase purity of the bulk crystal products. The few discrepancies in intensity between experimental and simulated values may be the consequence of preferred orientations of the crystal powder samples (see ESI†).

To rationalize the experimental observations, quantum chemical calculations were carried out on the model systems with the Gaussian09 suite of programs<sup>16</sup> at the SCS-MP2/SDD\*\* level of theory.<sup>17,18</sup> The reliability of SCS-MP2 method for the study of the weak molecular interactions can be found elsewhere.<sup>19</sup> SDD\*\* is the core basis sets (D95V for C, F and [2s3p] for I) augmented by two sets of polarization functions at carbons and halogens [(C, F, I) = 0.8, 0.25; 0.8, 0.25; 0.4, 0.07].<sup>20</sup> The structures of the complexes (Fig. 7) were optimized in the gas phase and the binding energies of the complexes were calculated using the supermolecule method. All binding energies reported are corrected for basis set superposition error using the counterpoise method of Boys and Bernardi.<sup>21</sup> The binding energies of the  $\pi\cdots\pi$  interactions and halogen bonds investigated in this study are shown in Fig. 7. It is noticed in Fig. 7 that the strengths of the  $\pi\cdots\pi$  interactions and halogen bonds are all larger than 5.30 kcal/mol. Let us add here that the binding energy of the  $\pi\cdots\pi$  interaction in the benzene dimer is just 2.78 kcal/mol.<sup>22</sup> More importantly, Fig. 7 clearly shows that the halogen bond in the dimer **1**⋯**1** is stronger than the  $\pi\cdots\pi$  interaction in the dimer **1**⋯**1** while the halogen bond in the dimer **2**⋯**2** is much weaker than the  $\pi\cdots\pi$  interaction in the dimer **2**⋯**2**. Based on the calculations, it appears that the strength of the halogen bond and the  $\pi\cdots\pi$  interaction is comparable in **1**, but the  $\pi\cdots\pi$  interaction is significantly stronger in the case of **2**. This is consistent with the observed crystal structures where the  $\pi\cdots\pi$  interaction is the primary force in the crystal structures obtained with compound **2**. Theoretical calculations explain the competition between  $\pi\cdots\pi$  interaction and halogen bond in the reported crystal structures.

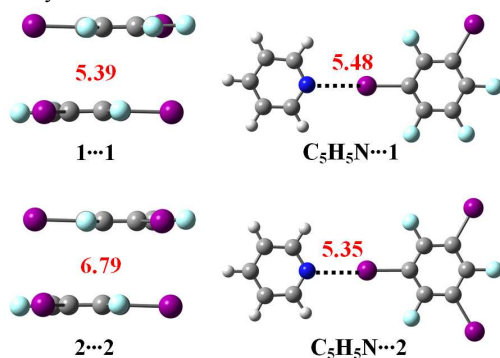


Fig. 7 Binding energies (red numbers; kcal/mol) of the  $\pi\cdots\pi$  interactions and halogen bonds investigated in this study.

## Conclusions

In this contribution, we have revealed that the  $\pi\cdots\pi$  interaction between two **1** molecules is unlikely to be very competitive for the strong C–I⋯N halogen bond while the  $\pi\cdots\pi$  interaction between two **2** molecules can successfully compete with the strong C–I⋯N halogen bond. As shown above, with the increasing of the number of iodine atoms, the  $\pi\cdots\pi$  interaction between two  $C_6F_xI_{(6-x)}$  ( $x = 0, 1, 2, 3, 4$  or  $5$ ) molecules becomes stronger. So it is expected that the  $\pi\cdots\pi$  interaction between two  $C_6F_xI_{(6-x)}$  ( $x = 0, 1$  or  $2$ ) molecules also can successfully compete with the strong C–I⋯N halogen bond. The corresponding cocrystallization reactions and calculations are in progress in our laboratory and will be reported in due course.

## Acknowledgements

The authors gratefully acknowledge financial support from the Natural Science Foundation of China (21072089, 21173113) and the science and technology innovation team support programs of Henan Province University (2012IRTSTHN019). This work is also partly supported by the Aid Project for the Leading Young Teachers in Henan Provincial Institutions of Higher Education of China (2010GGJS-166) and the Natural Science Foundation of Henan Educational Committee (2010A150017, 2011B150024).

## Notes and references

- <sup>a</sup> College of Chemistry and Chemical Engineering, Luoyang Normal University, Luoyang 471022, P. R. China. Fax: 86 379 65523821; Tel: 86 379 65523821; E-mail: lyhxxjbm@126.com
- <sup>b</sup> Northwest Agriculture and Forest University, Yangling 712100, P. R. China
- <sup>c</sup> Department of Chemistry, Zhengzhou University, Zhengzhou 450052, P. R. China
- † Electronic Supplementary Information (ESI) available: Cif files with X-ray powder diffraction patterns of cocrystals are presented as Supporting Information. See DOI: 10.1039/b000000x/
- 1 G. R. Desiraju, *Crystal Engineering: The Design of Organic Solids*, Elsevier, Amsterdam, 1989; (b) G. R. Desiraju and T. Steiner, *The Weak Hydrogen Bond In Structural Chemistry and Biology*, Oxford University Press, New York, 1997; (c) G. R. Desiraju, *Acc. Chem. Res.*, **1996**, *29*, 441–449.
- 2 (a) C. A. Hunter and J. K. M. Sanders, *J. Am. Chem. Soc.*, **1990**, *112*, 5525–5534; (b) C. A. Hunter, K. R. Lawson, J. Perkins and C. J. Urch, *J. Chem. Soc. Perkin Trans. 2*, **2001**, *5*, 651–669.
- 3 (a) P. Metrangolo, H. Neukirch, T. Pilati and G. Resnati, *Acc. Chem. Res.*, **2005**, *38*, 386–395; (b) P. Metrangolo, F. Meyer, T. Pilati, G. Resnati and G. Terraneo, *Angew. Chem. Int. Ed.*, **2008**, *47*, 6114–6127; (c) G. Cavallo, P. Metrangolo, T. Pilati, G. Resnati, M. Sansotera and G. Terraneo, *Chem. Soc. Rev.*, **2010**, *39*, 3772–3783; (d) R. Bertani, P. Sgarbossa, A. Venzo, F. Lejl, M. Amati, G. Resnati, T. Pilati, P. Metrangolo and G. Terraneo, *Coord. Chem. Rev.*, **2010**, *254*, 677–695; (e) E. Parisini, P. Metrangolo, T. Pilati, G. Resnati and G. Terraneo, *Chem. Soc. Rev.*, **2011**, *40*, 2267–2278.
- 4 (a) P. Metrangolo and G. Resnati, *Science*, **2008**, *321*, 918–919; (b) C. B. Aakeröy, M. Fasulo, N. Schultheiss, J. Desper and C. Moore, *J. Am. Chem. Soc.*, **2007**, *129*, 13772–13773; (c) E. Corradi, S. V. Meille, M. T. Messina, P. Metrangolo and G. Resnati, *Angew. Chem. Int. Ed.*, **2000**, *39*, 1782–1786; (d) N. Ma, Y. Zhang, B. Ji, A. Tian and W. Wang, *ChemPhysChem*, **2012**, *13*, 1411–1414; (e) A. Bauzá, D. Quiñero, A. Frontera and P. M. Deyá, *Phys. Chem. Chem. Phys.*, **2011**, *13*, 20371–20379.
- 5 H. Li, Y. Lu, Y. Liu, X. Zhu, H. Liu and W. Zhu, *Phys. Chem. Chem. Phys.*, **2012**, *14*, 9948–9955.
- 6 Y. Zhang, B. Ji, A. Tian and W. Wang, *J. Chem. Phys.*, **2012**, *136*, 141101.

[View Online](#)

- 7 T. X. Neenan and G. M. Whitesides, *J. Org. Chem.*, 1988, **53**, 2489–2496.
- 8 H. H. Wenk and W. Sander, *Eur. J. Org. Chem.*, 2002, **2002**, 3927–3935.
- 9 B. Ji, W. Wang, D. Deng and Y. Zhang, *Cryst. Growth Des.*, 2011, **11**, 3622–3628.
- 10 G. Marin, M. Andruh, A. M. Madalan, A. J. Blake, C. Wilson, N. R. Champness and M. Schröder, *Cryst. Growth Des.*, 2008, **8**, 964–975.
- 11 S. Hu, Z. S. Meng and M. L. Tong, *Cryst. Growth Des.*, 2010, **10**, 1742–1748.
- 12 (a) A. C. B. Lucassen, A. Karton, G. Leitus, L. J. W. Shimon, J. M. L. Martin and M. E. van der Boom, *Cryst. Growth Des.*, 2007, **7**, 386–392; (b) M. Vartanian, A. C. B. Lucassen, L. J. W. Shimon and M. E. van der Boom, *Cryst. Growth Des.*, 2008, **8**, 786–790; (c) B. M. Ji, D. S. Deng, N. Ma, S. B. Miao, X. G. Yang, L. G. Ji and M. Du, *Cryst. Growth Des.*, 2010, **10**, 3060–3069.
- 13 SHELXTL, Version 5.1; Bruker AXS: Madison, WI, 1998.
- 14 G. M. Sheldrick, 1997. SHELXL-97: program for the refinement of crystal structure, University of Göttingen, Germany.
- 15 P. Politzer, J. S. Murray and T. Clark, *Phys. Chem. Chem. Phys.*, 2010, **12**, 7748–7757.
- 16 M. J. Frisch, G. W. Trucks, H. B. Schlegel, G. E. Scuseria, M. A. Robb, J. R. Cheeseman, G. Scalmani, V. Barone, B. Mennucci, G. A. Petersson, H. Nakatsuji, M. Caricato, X. Li, H. P. Hratchian, A. F. Izmaylov, J. Bloino, G. Zheng, J. L. Sonnenberg, M. Hada, M. Ehara, K. Toyota, R. Fukuda, J. Hasegawa, M. Ishida, T. Nakajima, Y. Honda, O. Kitao, H. Nakai, T. Vreven, J. A. Montgomery, Jr., J. E. Peralta, F. Ogliaro, M. Bearpark, J. J. Heyd, E. Brothers, K. N. Kudin, V. N. Staroverov, T. Keith, R. Kobayashi, J. Normand, K. Raghavachari, A. Rendell, J. C. Burant, S. S. Iyengar, J. Tomasi, M. Cossi, N. Rega, J. M. Millam, M. Klene, J. E. Knox, J. B. Cross, V. Bakken, C. Adamo, J. Jaramillo, R. Gomperts, R. E. Stratmann, O. Yazyev, A. J. Austin, R. Cammi, C. Pomelli, J. W. Ochterski, R. L. Martin, K. Morokuma, V. G. Zakrzewski, G. A. Voth, P. Salvador, J. J. Dannenberg, S. Dapprich, A. D. Daniels, O. Farkas, J. B. Foresman, J. V. Ortiz, J. Cioslowski and D. J. Fox, *Gaussian09, Revision-A.02*, Gaussian, Inc., Wallingford, CT, 2009.
- 17 S. Grimme, *J. Chem. Phys.*, 2003, **118**, 9095–9102.
- 18 K. Pluháčková, P. Jurečka and P. Hobza, *Phys. Chem. Chem. Phys.*, 2007, **9**, 755–760.
- 19 K. E. Riley, J. A. Platts, J. Řezáč, P. Hobza and J. G. Hill, *J. Phys. Chem. A*, 2012, **116**, 4159–4169.
- 20 K. Pluháčková, P. Jurečka and P. Hobza, *Phys. Chem. Chem. Phys.*, 2007, **9**, 755–760.
- 21 S. F. Boys and F. Bernardi, *Mol. Phys.*, 1970, **19**, 553–566.
- 22 M. O. Sinnokrot and C. D. Sherrill, *J. Phys. Chem. A*, 2004, **108**, 10200–10207.

## Structural competition between $\pi\cdots\pi$ interaction and halogen bond: a crystallographic study

Baoming Ji, Weizhou Wang, Dongsheng Deng, Yu Zhang, Lei Cao, Le Zhou, Chuansheng Ruan and Tiesheng Li

The structural competition between  $\pi\cdots\pi$  interaction and halogen bond is directly observed in six designed cocrystals.

